Condensed Matter and Interphases

Original articles

The effect of current density on the structure of nickel electrolytic foams and their catalytic properties during hydrogen production

T. S. Trofimova✉, T. N. Ostanina, V. M. Rusoi, E. A. Mazurina

*Ural Federal University,
19 Mira str., Ekaterinburg 620002, Russian Federation*

Abstract

The effect of current density on the regularities of nickel foam deposition processes has been studied. Porous nickel foams were obtained by electrochemical deposition in the galvanostatic mode at current densities of 0.3, 0.6, 0.9, and 1.2 A cm^{-2}. The obtained deposits were characterized by high porosity and well adherence to the substrate material. The electrolytic foams had macro- and micropores.

The features of the formation of the macropore system have been studied. It has been established that at low hydrogen evolution rates, a gradual formation of a porous structure occurs. While at higher rates, the formation of the matrix structure ends in the first minutes of electrolysis. It was shown that the log-normal distribution can be used to describe the formation of a hydrogen template as a system of macropores in electrolytic nickel foams over a wide range of current densities. A technique for the estimation of nickel foam macroporosity based on the data on the fraction of the surface occupied by macropores is proposed. The total porosity of deposits was calculated based on the data on the mass and volume of electrolytic foams. The catalytic activity of the obtained porous electrodes towards the hydrogen evolution reaction was analysed in an alkali solution. The value of depolarization at a current density of 0.3 A·cm^{-2} was used as a criterion for the efficiency of nickel foams. The value of depolarization for the obtained deposits varies in a wide range from 170 to 400 mV and strongly depends on the conditions of foam synthesis and their thickness.

It has been established that nickel foams obtained at 1.2 A·cm^{-2} exhibit the best catalytic properties due to their uniform structure characterized by a large number of macropores evenly distributed throughout the foam volume. This ensures maximum access of the reacting particles to the electrode surface.

Keywords: Porosity, Nickel, Electrodeposition, Catalytic properties, Depolarization

✉ Tina-Tini S. Trofimova, e-mail: t.s.kuloshvili@urfu.ru

Condensed Matter and Interphases / Конденсированные среды и межфазные границы   2023;25(1): 139–148

T. S. Trofimova et al.   The effect of current density on the structure of nickel electrolytic foams...

1. Introduction

Water electrolysis is a promising method for producing hydrogen due to the sufficient simplicity of the technology and the possibility of introducing "green" technologies into this process [1]. However, electrolysis is a relatively energy-intensive process. A significant contribution to energy losses is made by hydrogen and oxygen evolution reaction overpotentials. One of the ways to increase the efficiency of electrode processes is to use electrodes with a developed surface. In this case, porous electrodes are used, which have a large surface area compared to smooth electrodes. Due to the large fraction of the active surface, a decrease in the real current density, and, accordingly, overvoltage, is achieved.

Metal foams are porous electrodes possessing all properties of electrocatalytic electrodes. They are characterized by their high porosity and large available surface area, high mechanical strength, and good conductivity. The synthesis of porous metal electrodes is carried out by using the dynamic hydrogen bubble template method [2–6]. The formation of a porous structure occurs due to the crystallization of the metal around the hydrogen bubbles under conditions of high current densities, when metal ion reduction is accompanied by hydrogen evolution. In this case, part of the electrode surface is covered with gas bubbles, and the metal crystallizes in the form of branched dendrites on free surface areas. It is known that this method is used to obtain nickel [7, 8], cobalt [9, 10], copper foams [11, 12], as well as foams of their alloys [13–16].

The main advantage of the electrochemical deposition is the possibility of controlling the foam structure by changing the electrolysis conditions. The structure of the foams, in turn, affects their catalytic properties.

The literature usually contains a description of the morphological features of porous deposits [3,4,7,8,10] and does not provide quantitative patterns describing the process of formation of a system of large pores and a dendrite metal deposit between them. In a previous article [17], the main provisions of a phenomenological model that describe the process of the formation of nickel foams and allow to calculate the change in foam porosity during electrodeposition were proposed. The model is based on empirical regularities that describe the time-dependent change in the deposit growth rate, metal current efficiency, and the fraction of the outer surface occupied by large pores. The applicability of the previously proposed empirical equations for the quantitative description of nickel foam electrodeposition in a wide range of current densities for subsequent forecasting of the conditions for the synthesis of foams with desired properties is of interest.

The purpose of this study was investigation of the effect of current density on the regularities of nickel foam deposition, the formation of a system of large pores, and the catalytic properties of deposits with respect to the hydrogen evolution reaction.

2. Experimental

Nickel foams were prepared from a chloride electrolyte [18] containing 0.2 M $NiCl_2$ and 2 M NH_4Cl (pH = 3.2) in galvanostatic mode at current densities of 0.3, 0.6, 0.9, and 1.2 A·cm^{-2} per geometric surface of the electrode. Foams were produced within 1, 2, 3, 4, 5, 10, and 15 minutes at each current density. Three parallel experiments were carried out at each point. The working electrode was a copper plate, on the surface of which a nickel layer with the thickness of 9 μm was preliminarily deposited from a Watts electrolyte containing 280 g·l^{-1} $NiSO_4$·$7H_2O$, 50 g·l^{-1} NaCl, 35 g·l^{-1} H_3BO_3 at a current density of 0.015 A cm^{-2}. The area of the working surface of the electrode with nickel coating before the deposition of foam was 1 cm^2. Nickel foil was used as an auxiliary electrode. Autolab PGSTAT 302N electrochemical station (Metrohm Autolab AG, the Netherlands) was used for the deposition of foams and investigation of their catalytic properties. After deposition, the samples were thoroughly washed in distilled water and dried in air. Samples obtained at current densities of 0.3, 0.6, 0.9, and 1.2 A cm^{-2} are denoted in the study as 0.3Ni, 0.6Ni, 0.9Ni, and 1.2Ni, respectively. The mass of foams was determined by weighing with an accuracy up to four decimal places using LA 310S analytical balance (Sartorius, Germany). The total porosity was calculated taking into account the volume of foams.

Condensed Matter and Interphases / Конденсированные среды и межфазные границы 2023;25(1): 139–148

T. S. Trofimova et al. The effect of current density on the structure of nickel electrolytic foams...

Surface morphology was analysed using an Olympus BX51 optical microscope (Olympus, Japan) and a Tescan VEGA 4 scanning electron microscope (SEM) (TESCAN, Czech Republic). The thickness of nickel deposits (h) was evaluated based on photo images of a thin section of the electrode cross section with a deposit.

The catalytic efficiency of the electrodes in relation to the hydrogen evolution reaction was evaluated by the analysis of the cathodic polarization curves obtained in 1 M NaOH solution at a potential scan rate of 3 mV·s⁻¹. The resulting electrolytic foam was the working electrode, and a graphite rod was used as the counter electrode. The potential was measured relative to a saturated silver chloride reference electrode. At least 3 curves were taken for each electrode until reproducible results were obtained. All studies were carried out at a temperature of 25°C.

3. Results and discussion

3.1. Morphology of nickel foams

Nickel electrolytic foams are characterized by the presence of macro- and micropores (Fig. 1). Macropores were formed in places where the electrode surface is shielded by hydrogen bubbles and mainly represented by through-channels (Fig. 1e), the exits of channels to the foam surface are clearly visible on microphotographs (Fig. 1a–d).

Under the studied conditions, the metal was deposited as branched dendrites. The space between the dendrite branches and individual dendrites is a branched system of voids, with size much smaller than the size of macropores, and it can be called microporosity.

During 15 minutes of electrolysis at all current densities, the nickel foam thickness (h) increased linearly with the deposition time
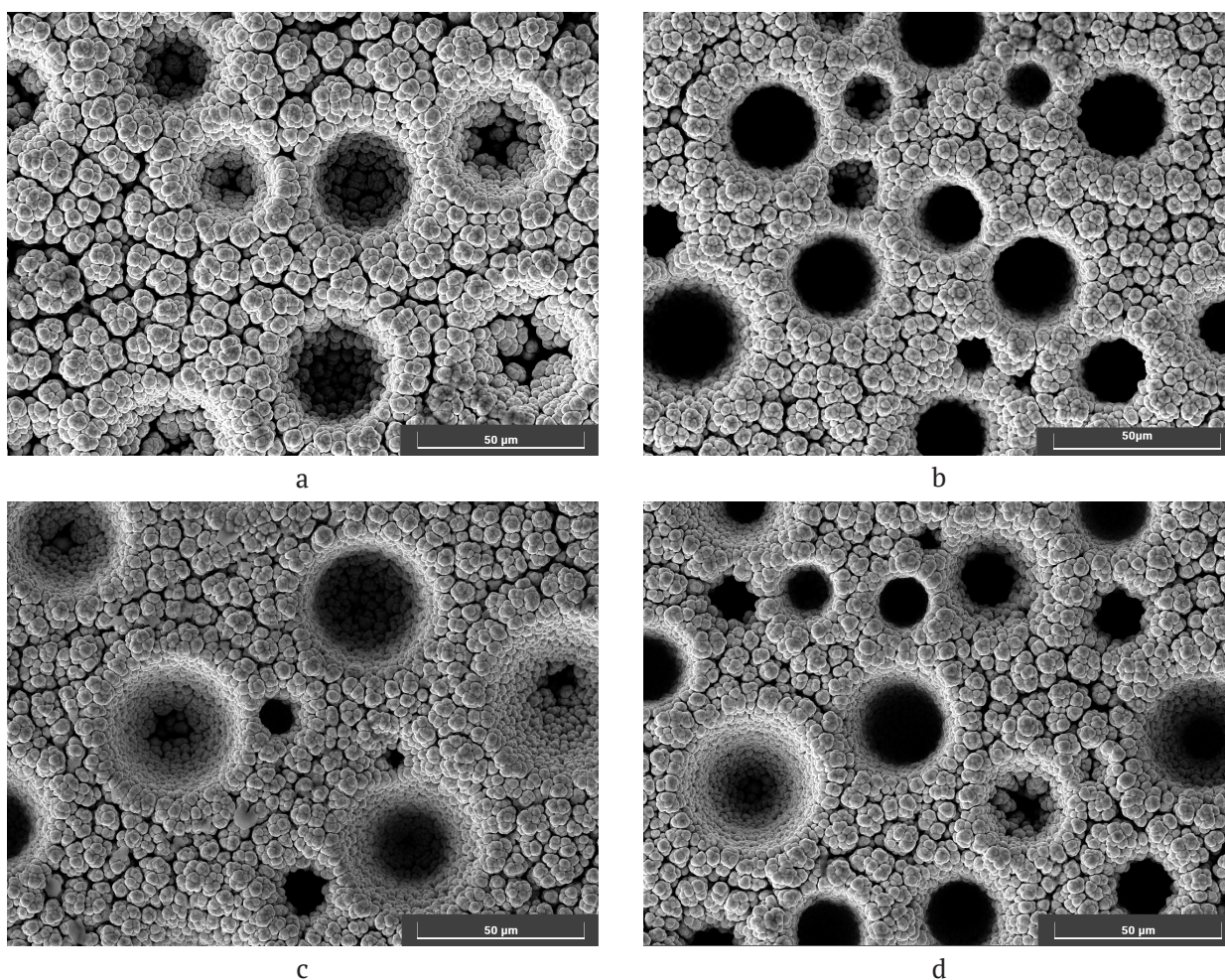
Fig. 1. SEM images of foams obtained at i = 0.3 (a), 0.6 (b), 0.9 (c), and 1.2 (d) A·cm⁻²; t = 10 min. Image of the macropore on a foam cross section (d)

Condensed Matter and Interphases / Конденсированные среды и межфазные границы   2023;25(1): 139–148

T. S. Trofimova et al.   The effect of current density on the structure of nickel electrolytic foams...

(Fig. 2). At the same time, the deposition growth rate (dh/dt) increased with increase in current density (Table 1).

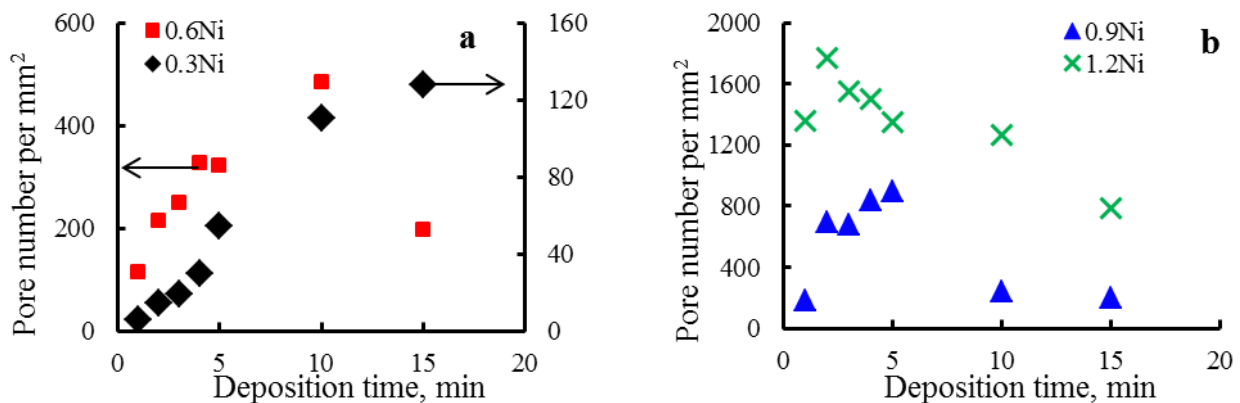**Table 1.** The effect of current density on the dendrite elongation rate and their radius

Deposition current density, $A \cdot cm^{-2}$	dh/dt, cm/min	r_{tip}, µm
0.3	$0.64 \cdot 10^{-3}$	5.35
0.6	$0.97 \cdot 10^{-3}$	3.50
0.9	$1.07 \cdot 10^{-3}$	3.38
1.2	$1.25 \cdot 10^{-3}$	2.73

It is known [19] that, under conditions of diffusion limitations, metal deposition proceeds at the dendrite tips located at the deposit growth front, and the elongation rate (dh/dt) (Fig. 2) is determined by the limiting diffusion current density of spherical diffusion (i_{tip}) [19]:

$$\frac{dh}{dt} = \frac{\vartheta_{Ni}}{zF} i_{tip},\qquad(1)$$
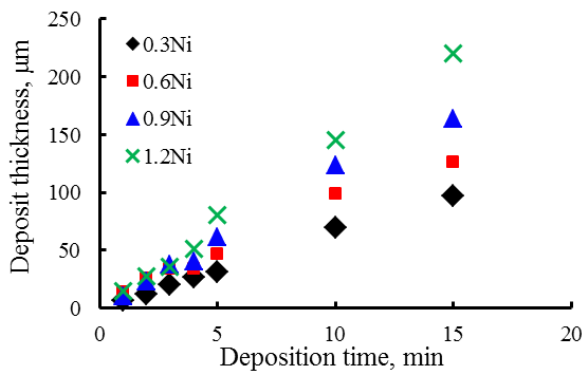
Fig. 2. Dependence of nickel foam thickness on deposition time at current density of 0.3, 0.6, 0.9, and 1.2 A of 0.3, 0.6, 0.9, and 1.2 A·cm⁻²
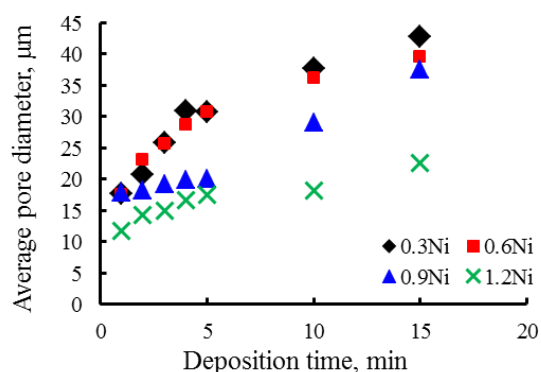
$$i_{tip} = \frac{zFDC}{r_{tip}},\qquad(2)$$

where ϑ_{Ni} is molar volume of metal, $m^3 \cdot mol^{-1}$, D is the diffusion coefficient of nickel ions, $m^2 \cdot s^{-1}$, C is concentration of nickel ions in solution, $mol \cdot m^{-3}$, dh/dt is the rate of dendrite elongation, $m \cdot s^{-1}$.

The radius of dendrite branches was determined based on the deposit growth rate:

$$r_{tip} = \frac{DC \cdot \vartheta_{Me}}{dh/dt}.\qquad(3)$$

As follows from the literature data [19], the constancy of the growth rate during electrolysis indicates the formation of a dendrite deposit, characterised by uniform structure throughout the thickness. The calculated values of the tip radii decrease with increase in current density (Table 1) from 5.35 to 2.73 µm, which, as will be shown below, affects the microporosity of the foams.

Photographs of the outer surface of nickel foams obtained using an Olympus BX51 optical microscope (Olympus, Japan) were used to determine the diameter and number of macropores (Figs. 3 and 4). At least three samples obtained under the same conditions were analysed and at least 5 sites were selected on each of them. With an increase in the current density, an increase in the number of macropores per unit surface and a decrease in their average diameter were observed, which is consistent with the literature data [7, 11, 20]. Such dependences are explained by an increase in the rate of hydrogen evolution and, accordingly,

Fig. 3. Change of macropore number at current densities of 0.3 and 0.6 A·cm⁻² (a), 0.9 and 1.2 A·cm⁻² (b)

Condensed Matter and Interphases / Конденсированные среды и межфазные границы   2023;25(1): 139–148

T. S. Trofimova et al.   The effect of current density on the structure of nickel electrolytic foams…

Fig. 4. Change of macropore diameters at current densities of 0.3, 0.6, 0.9, and 1.2 A·cm⁻²

by a decrease in the residence time of a bubble on the deposit surface.

At current densities of 0.3 and 0.6 A·cm⁻² within 10 minutes, an increase in the number of large pores up to 400 mm was observed⁻² (Fig. 3a), which indicates the gradual formation of a porous structure. With an increase in current density up to 1.2 A·cm⁻², the formation of the template structure (formation of macropores more than 1600 mm⁻²) finished within the first 2 minutes of electrolysis, then within 10 minutes the number of macropores decreased, but remained very high (Figs. 3b and 4). A similar pattern was observed for 0.9Ni samples, but for 5 minutes. With further electrolysis, there was a significant decrease in the number of pores and an increase in their size.

The difference in the dynamics of the formation of the macropore structure was associated with the intensity of hydrogen evolution. At low rates of hydrogen evolution, gas bubbles retained on the electrode surface for a time sufficient for their coalescence; therefore, for low current densities, the dependence of the number of pores and their sizes on the deposition time was observed. At high rates of hydrogen evolution, the bubbles quickly reached the critical diameter and immediately detached from the surface; therefore, the structure of the foams was more stable and changes less with time.

3.2. Determination of porosity

When metal foams are used as electrodes, the thickness of the porous layer and the fraction of the surface involved in the electrochemical process are important. Since the deposition rate

significantly depends on the current density, it is important to reveal how the structural properties change not with the deposition time, but with the thickness of the foams.

For deposits with different thickness obtained over different times, the fraction of the surface occupied by macropores θ_{macro} was calculated [17,21]. For calculations, several sites (K) on the electrode surface with deposits with the same area (s) were isolated. The total number of pores (N_k) and the diameter of each macropore (d_{jk}) were determined for each site. The fraction of the outer surface of the deposit occupied by macropores was estimated as follows:

$$\theta_{macro}(h) = \frac{\sum_{k=1}^{K}\sum_{j=1}^{N_k}\pi\frac{d_{jk}^2}{4}}{K \cdot s}. \quad (4)$$

According to the experimental data presented in Figs. 5, the dependence $\theta_{macro}(h)$ has a maximum, which is in good agreement with the data on changes in the number and diameter of macropores on time (Figs. 3 and 4). An increase in the fraction of the surface occupied by macropores was associated with an increase in the number of macropores and their diameter, and a decrease θ_{macro} occurred due to the merging of macropores.

The process of macropore formation is stochastic, therefore, for the approximation of the dependence of the fraction of large pores on the deposit thickness, a log-normal distribution was used [22]:

$$\theta_{macro}(H) = \frac{a}{\sigma\sqrt{2\pi}}\frac{1}{H}\exp\left[-\frac{1}{2\sigma^2}\left(\ln(H)-\mu\right)^2\right]. \quad (5)$$

Here σ and μ are distribution parameters, a is the scaling factor. Function argument $H = h/h_{st}$ is dimensionless, since the deposit thickness is divided by the unit of measurement $h_{st} = 1$ μm. Calculation of the σ, μ, a values was carried out by minimizing the sum of squared deviations of the experimental data θ_{macro} from data calculated by equation (5) [21]. The values of the determined coefficients are presented in Table 2.

As can be seen from the Table 2, the distribution parameters (σ and μ) for all porous deposits were close by the order of magnitude and regularly changed with increase in current density. The physical meaning of the parameters is still unclear, but it is important that the log-

Condensed Matter and Interphases / Конденсированные среды и межфазные границы   2023;25(1): 139–148

T. S. Trofimova et al.   The effect of current density on the structure of nickel electrolytic foams...

Table 2. The values of the empirical coefficients of Eq. 10 and the determination coefficient

Deposit	Coefficients and R^2			
	a	σ	μ	R^2
0.3 Ni	72.24	0.81	5.50	0.994
0.6 Ni	73.00	0.87	5.10	0.995
0.9 Ni	87.26	0.91	5.09	0.996
1.2 Ni	99.22	1.00	5.09	0.990

normal distribution describes well the change in the fraction of the surface occupied by macropores in a wide range of current densities. This indicates the similarity of the mechanisms of macropore formation, as well as the invariance of this mechanism with an increase in the current density of foam deposition. The good agreement of the experimental values of the fraction of macropores (Fig. 5) with the values calculated using the approximating equation 5 indicates the stochastic nature of the process of formation of the macropore system.

The total porosity was determined taking into account the mass (m_{Ni}) and volume of porous deposit (V_{dep}):

$$\beta_\Sigma = \frac{V_{pore}}{V_{dep}} = 1 - \frac{m_{Ni}}{\rho_{Ni} \cdot V_{dep}}, \qquad (6)$$

where V_{dep} – overall volume of deposit, ρ_{Ni} is the density of nickel. $V_{dep} = S_{geom} \cdot h$, S_{geom} is the geometric area of the deposit surface, cm^2; V_{pore} is the volume of all pores in the deposit. The values of total porosity for deposits of different thicknesses are presented in Table 3.
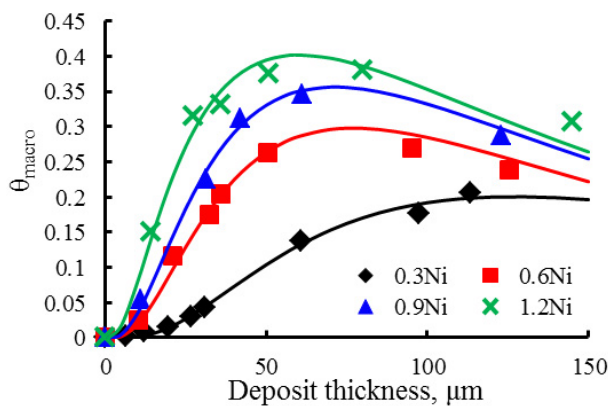
Fig. 5. Change of the θ_{macro} over the deposit thickness at i = 0.3, 0.6, 0.9, and 1.2 A·cm^{-2}. Markers – experimental data, lines – approximation by Eq. 5

Macroporosity is the ratio of the volume of large pores V_{macro} to deposit volume V_{dep}:

$$\beta_{macro} = \frac{V_{macro}}{V_{dep}}. \qquad (7)$$

The pore volume is the product of the cross-sectional area of the macropores at the deposit growth front (S_{macro}) and their depth. As can be seen from the micrograph (Fig. 1e), the macropores were through-pores; therefore, the average pore depth was taken as the thickness of the deposit layer (h):

$$V_{macro} = S_{macro} \cdot h. \qquad (8)$$

The macropore diameter varied with the deposit thickness. At the same time the porosity of the deposit changed. Therefore V_{macro} for deposits of different thickness was determined based on the experimental values $S_{macro,i} = \theta_{macro,i} \cdot S_{geom}$ using numerical integration of the dependence of the area of macropores on the thickness of the foam according to the equation:

$$V_{macro} = \sum_{i=1}^{M} \left[\frac{\left(S_{macro_i} + S_{macro_{i+1}}\right) \cdot \left(h_{i+1} - h_i\right)}{2} \right], \qquad (9)$$

here h_i is thickness of i-th deposit, μm; i = 0...M is foam sample number, M is quantity of deposit samples with different thicknesses obtained for different electrolysis times. At i = 0 electrolysis time was 0, respectively, h_i = 0 and S_{macro_i} = 0.

Macroporosity, as the proportion of macropores in the deposit volume, was determined:

$$\beta_{macro} = \frac{V_{macro}}{S_{geom} \cdot h}. \qquad (10)$$

The macroporosity for nickel foams of different thicknesses, calculated based on the experimental data, are represented by markers in Fig.6 and in Table 3. Macroporosity increased

Table 3 Values of total, macro- and microporosity of electrolytic foams obtained at current densities of 0.3, 0.6, 0.9, and 1.2 A·cm^{-2} for 15 minutes

Deposit	β_Σ, %	β_{macro}, %	β_{micro}, %
0.3 Ni	62.9	9.1	53.8
0.6 Ni	49.2	19.4	29.9
0.9 Ni	47.3	26.6	20.7
1.2 Ni	41.6	31.1	10.5

Condensed Matter and Interphases / Конденсированные среды и межфазные границы   2023;25(1): 139–148

T. S. Trofimova et al.   The effect of current density on the structure of nickel electrolytic foams...

significantly with increase in foam deposition current density.

Taking into account the determined coefficients a, σ and μ (Table 2), the numerical integration of log-normal dependences was carried out $\theta_{macro}(H)$, and it allowed to calculate the volume of large pores for any deposit thickness:

$$V_{macro} = \int_0^h S_{macro}(h)dh = \int_0^h S_{geom} \cdot \theta_{macro}(h)dh. \quad (11)$$

Taking into account equation (10) macroporosity is:

$$\beta_{macro} = \frac{1}{h}\int_0^h \theta_{macro}(h)dh. \quad (12)$$

As can be seen in Fig. 6, the calculated curves are in good agreement with the values β_{macro} obtained based on experimental data, which indicates the applicability of equation 5 for describing the process of formation of the porous structure of nickel foams.

It should be noted that the total porosity of the foams was much higher than the macroporosity, which is due only to the presence of channels for the release of hydrogen bubbles. Total porosity also includes microporosity. It is not possible to determine the shape and size of microvoids, but it is possible to estimate their fraction, microporosity. Microporosity was calculated as the difference between the total porosity and macroporosity of deposits $\beta_{micro} = \beta_{\Sigma} - \beta_{macro}$.

The results of calculations of the total porosity, macroporosity, and microporosity for foams obtained at different current densities after 15 minutes of electrolysis are presented in Table 3. It can be seen that the total porosity of the foams gradually decreased with increasing deposition current density. In this case, the fraction of macropores and their contribution to the total porosity increased significantly, and microporosity decreased. The decrease in microporosity was associated with an increase in the number of dendrite branches on the foam surface between large pores, which led to their more compact arrangement. This conclusion is confirmed by the analysis of micrographs of samples using SEM (Fig. 1). The combination of macro- and microporosity provides the
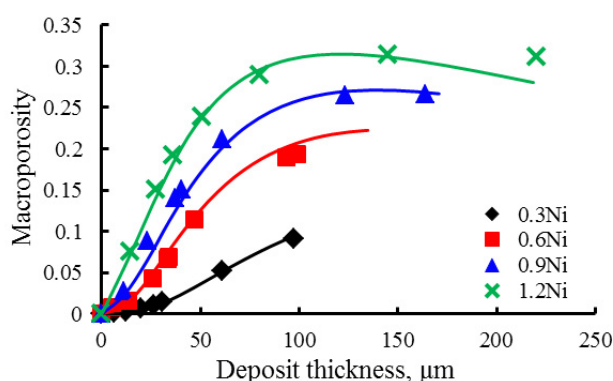

Fig. 6. Change of microporosity over the deposit thickness at i = 0.3, 0.6, 0.9, and 1.2 A·cm^{-2}. Markers – experimental data, lines – calculation by Eq. 12.
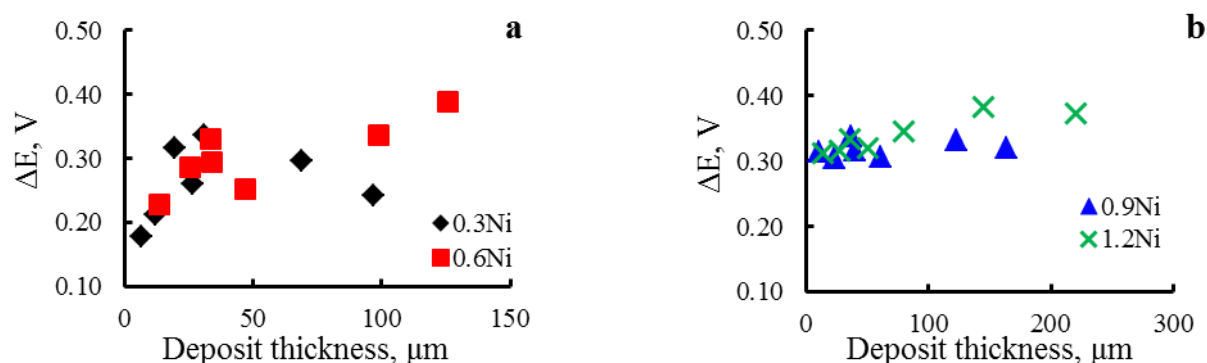
high efficiency of nickel foams as electrode materials.

3.3. Assessment of catalytic properties

For the evaluation of the catalytic properties of nickel foams with respect to the hydrogen evolution reaction, cathodic polarization curves were recorded in a 1 M NaOH solution. The polarization curves obtained on porous deposits were shifted to more positive potentials compared to the smooth nickel electrode.

The depolarization was chosen as a criterion of catalytic properties. The depolarization value is the difference in the potentials of the porous (E_{dep}) and a smooth nickel electrode (E_{sm}): $\Delta E = E_{dep} - E_{sm}$ at current density i = 0.3 A·cm^{-2}. This current density is used in the electrolysis of water in alkaline electrolytic cells [23].

As can be seen from Fig. 7, the depolarization of hydrogen evolution process varies in the range from 170 to 400 mV, depending on the mode of the production of foams and their thickness. The catalytic properties of the 0.3Ni and 0.6Ni samples strongly depend on the deposit thickness (Fig. 7a). This fact can be explained by the heterogeneity of the foam structure over the thickness: the number of pores and their sizes vary within a fairly wide range, which affects the surface area available for the hydrogen evolution reaction. As was shown above, 0.9Ni and 1.2Ni samples were characterized by the presence of a regular pore structure with a low variation of thickness. Due to this, their catalytic properties were quite stable and did not depend on the thickness of the deposit. In general, the good catalytic properties

Condensed Matter and Interphases / Конденсированные среды и межфазные границы   2023;25(1): 139–148

T. S. Trofimova et al.   The effect of current density on the structure of nickel electrolytic foams...

Fig. 7. Dependence of hydrogen evolution depolarization in 1 M NaOH at $i = 0.3$ A·cm^{-2} on the deposit thickness for 0.3Ni and 0.6Ni (a), 0.9Ni and 1.2Ni (b) samples

of the 0.9Ni and 1.2Ni samples can be explained by the high macroporosity, which makes a large part of the electrode surface accessible for the HER reaction.

4. Conclusion

It was shown that within 15 minutes of electrolysis, the growth rate of nickel foams remains constant and increased with increase in current density.

It has been established that at low current densities, a gradual formation of a porous structure occurred, which led to inhomogeneity in the size and number of pores throughout the thickness of the deposit. At the same time, at high current densities, the formation of the template structure ends in the first minutes of electrolysis and after the fraction of the surface occupied by macropores remained high.

It was shown that the log-normal distribution can be used to describe the formation of a hydrogen template as a system of macropores in electrolytic nickel foams in a wide range of current densities.

The macroporosity of deposits increased, while the total porosity and the fraction of micropores decreased with a change in the deposition current density from 0.3 to 1.2 A·cm^{-2}, which improves the catalytic properties of deposits.

Catalytic properties with respect to the hydrogen evolution reaction in an alkali solution for deposits obtained at current densities of 0.9 and 1.2 A·cm^{-2}, remained high at any foam thickness due to the formation of a more uniform porous structure of deposits with a high number of large pores of small diameter.

Contribution of the authors

The authors contributed equally to this article.

Conflict of interests

The authors declare that they have no known competing financial interests or personal relationships that could have influenced the work reported in this paper.

References

1. Li X., Zhao L., Yu J., Liu X., Zhang X., Liu H., Zhou W. Water splitting: from electrode to green energy system. *Nano-Micro Letters*. 2020;12: 131. https://doi.org/10.1007/s40820-020-00469-3

2. Herraiz-Cardona I., Ortega E., Vázquez-Gómez L., Pérez-Herranz V. Double-template fabrication of three-dimensional porous nickel electrodes for hydrogen evolution reaction. *International journal of hydrogen energy*. 2012;37(3): 2147–2156. https://doi.org/10.1016/j.ijhydene.2011.09.155

3. Siwek K. I., Eugenio S., Santos D. M. F., Silva M. T., Montemor M. F. 3D nickel foams with controlled morphologies for hydrogen evolution reaction in highly alkaline media. *International journal of hydrogen energy*. 2019;44(3): 1701–1709. https://doi.org/10.1016/j.ijhydene.2018.11.070

4. Swain N., Mitra A., Saravanakumar B., Balasingam S. K., Mohanty S., Nayak S. K., Ramadoss A., Construction of three-dimensional MnO$_2$/Ni network as an efficient electrode material for high performance supercapacitors. *Electrochimica Acta*. 2020;342: 136041. https://doi.org/10.1016/j.electacta.2020.136041

5. Shi Y., Zhang L., Zhang Y., Li J., Fu Q., Zhu X., Liao Q. Construction of a hierarchical porous surface composite electrode by dynamic hydrogen bubble template electrodeposition for ultrahigh-performance thermally regenerable ammonia-based batteries.

Condensed Matter and Interphases / Конденсированные среды и межфазные границы   2023;25(1): 139–148

T. S. Trofimova et al.   The effect of current density on the structure of nickel electrolytic foams...

Chemical Engineering Journal. 2021;423: 130339. https://doi.org/10.1016/j.cej.2021.130339

6. Qiu, H., Tang, T., Asif, M., Huang, X., Hou, Y. 3D porous Cu current collectors derived by hydrogen bubble dynamic template for enhanced Li metal anode performance. *Advanced Functional Materials.* 2019;29: 1808468. https://doi.org/10.1002/adfm.201808468

7. Yu X., Yuan Z. The structure evolution mechanism of Ni films depending on hydrogen evolution property during electrodeposition process. *Metallurgical and Materials Transactions B.* 2019;50: 587–594. https://doi.org/10.1007/s11663-019-01512-4

8. Sengupta S., Patra A., Jena S., Das K., Das S. A study on the effect of electrodeposition parameters on the morphology of porous nickel electrodeposits. *Metallurgical and Materials Transactions A.* 2018;49: 920–937. https://doi.org/10.1007/s11661-017-4452-8

9. González-Buch C., Herraiz-Cardona I., Ortega E., García-Antón J., Pérez-Herranz V. Synthesis and characterization of macroporous Ni, Co and Ni–Co electrocatalytic deposits for hydrogen evolution reaction in alkaline media. *International Journal of Hydrogen Energy.* 2013;38(25): 10157–10169. https://doi.org/10.1016/j.ijhydene.2013.06.016

10. Vainoris M., Tsyntsaru N., Cesiulis H. Modified electrodeposited cobalt foam coatings as sensors for detection of free chlorine in water. *Coatings.* 2019;9: 306. https://doi.org/10.3390/coatings9050306

11. Zhang H., Ye Y., Shen R., Ru Ch., Hu Y. Effect of bubble behavior on the morphology of foamed porous copper prepared via electrodeposition. *Journal of The Electrochemical Society.* 2013;160: D441. https://doi.org/10.1149/2.019310jes

12. Cui L., Hu L., Shen Q., Liu X., Jia H., Xue J. Three-dimensional porous Cu_2O with dendrite for efficient photocatalytic reduction of CO_2 under visible light. *Applied Surface Science.* 2022;581: 152343. https://doi.org/10.1016/j.apsusc.2021.152343

13. Teng X., Wang J., Ji L., Liu Y., Zhang C., Chen Z. Fabrication of three-dimensional multiscale porous alloy foams at a planar substrate for efficient water splitting. *ACS Sustainable Chemistry & Engineering.* 2019;7(5): 5412–5419. https://doi.org/10.1021/acssuschemeng.8b06452

14. Eugénio S., Demirci U. B., Silva T. M., Carmezim M. J., Montemor M. F. Copper-cobalt foams as active and stable catalysts for hydrogen release by hydrolysis of sodium borohydride. *International Journal of Hydrogen Energy.* 2016;41(20): 8438–8448. https://doi.org/10.1016/j.ijhydene.2016.03.122

15. Swain N., Saravanakumar B., Mohanty S., Ramadoss A., Engineering of thermally converted 3D-$NiOCo_3O_4$/Ni//3D-Υ-Fe_4NC@Ni/SS porous electrodes for high-performance supercapatteries. *Electrochimica Acta.* 2022;412: 140076. https://doi.org/10.1016/j.electacta.2022.140076

16. Mirzaee M., Dehghanian Ch. Nanostructured Ni-Cu foam electrodepositedon a copper substrate applied as supercapacitor electrode. *Acta Metallurgica Slovaca.* 2018;24: 325–336. https://doi.org/10.12776/ams.v24i4.1138

17. Trofimova T. S., Ostanina T. N., Nikitin V. S., Rudoi V. M., Ostanin N. I., Trofimov A. A. Modeling of the porous nickel deposits formation and assessing the effect of their thickness on the catalytic properties toward the hydrogen evolution reaction. *International Journal of Hydrogen Energy.* 2021;46: 16857–16867. https://doi.org/10.1016/j.ijhydene.2021.02.093

18. Marozzi C. A., Chialvo A. C. Development of electrode morphologies of interest in electrocatalysis. Part 1: Electrodeposited porous nickel electrodes. *Electrochimica Acta.* 2000;45: 2111–2120. https://doi.org/10.1016/S0013-4686(99)00422-3

19. Diggle J. W., Despic A. R., Bockris J. O. The mechanism of the dendritic electrocrystallization of zinc. *Journal of The Electrochemical Society.* 1969;116: 1503. https://doi.org/10.1149/1.2411588

20. Eugénio S., Silva T. M., Carmezim M. J., Duarte R. G., Montemor M. . Electrodeposition and characterization of nickel-copper metallic foams for application as electrodes for supercapacitors. *Journal of Applied Electrochemistry.* 2014;44: 455–65. https://doi.org/10.1007/s10800-013-0646-y

21. Trofimova T. S., Darintseva A. B., Ostanina T. N., Rudoi V. M., Il'ina I.E. Effect of the structure and morphology of Ni-based porous deposits on their electrocatalytic activity towards hydrogen evolution reaction. *Powder Metallurgy and Functional Coatings.* 2021;(4): 57–67. (In Russ., abstract in Eng.). https://doi.org/10.17073/1997-308X-2021-4-57-67

22. Eadie W. T., Dryard D., James F. E., Roos M., Sadoulet B. *Statistical methods in experimental physics.* North-Holland, Amsterdam; 1971. 296 p.

23. Bernäcker C. I., Rauscher T., Büttner T., Kieback B., Röntzsch L. A Powder metallurgy route to rroduce raney-nickel electrodes for alkaline water electrolysis. *Journal of The Electrochemical Society.* 2019;166(6): F357–F363. https://doi.org/10.1149/2.0851904jes

Information about the authors

Tina-Tini S. Trofimova, Junior Researcher Scientific of the Laboratory of Electrochemical Devices and Materials, Institute of Chemical Engineering, Ural Federal University (Ekaterinburg, Russia).

https://orcid.org/0000-0002-4135-8856
t.s.kuloshvili@urfu.ru

Condensed Matter and Interphases / Конденсированные среды и межфазные границы   2023;25(1): 139–148

T. S. Trofimova et al.   The effect of current density on the structure of nickel electrolytic foams...

Tatiana N. Ostanina, Dr. Sci. (Chem.), Professor of the Technology of Electrochemical Manufactures Department, Institute of Chemical Engineering, Ural Federal University (Ekaterinburg, Russia).

https://orcid.org/0000-0002-6149-7204

t.n.ostanina@urfu.ru

Valentin M. Rudoi, Dr. Sci. (Chem.), Professor of the Technology of Electrochemical Manufactures Department, Institute of Chemical Engineering, Ural Federal University (Ekaterinburg, Russia).

https://orcid.org/0000-0002-8055-8148

v.m.rudoi@urfu.ru

Elizaveta A. Mazurina, Master's Degree student of the Technology of Electrochemical Manufactures Department, Institute of chemical engineering, Ural Federal University (Ekaterinburg, Russia).

https://orcid.org/0000-0001-5507-0311

maz_liza@mail.ru